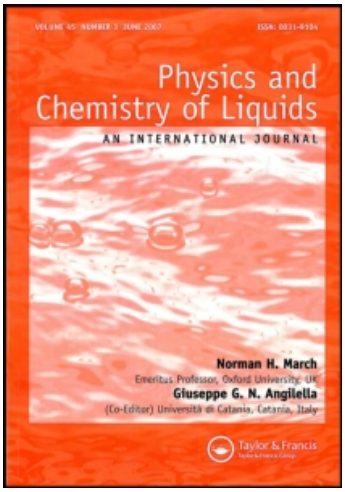

Physics and Chemistry of Liquids
Publication details, including instructions for authors and subscription information:
http://www.informaworld.com/smpp/title~content=t713646857

Influence of temperature on ultrasonic velocity measurements of ethanol + water + ethyl acetate mixtures

J. M. Resa[a]; C. González[a]; J. M. Goenaga[a]; M. Iglesias[b]
[a] Departamento de Ingeniería Química, Universidad del Pais Vasco, Vitoria, España [b] Departament d'Enginyeria Química, Escola Tècnica Superior d'Enginyeria Química, Universitat Rovira i Virgili, Avinguda Països Catalans 26, 43007 Tarragona, España

To cite this Article Resa, J. M. , González, C. , Goenaga, J. M. and Iglesias, M.(2005) 'Influence of temperature on ultrasonic velocity measurements of ethanol + water + ethyl acetate mixtures', Physics and Chemistry of Liquids, 43: 1, 65 — 89
To link to this Article: DOI: 10.1080/00319100512331323977
URL: http://dx.doi.org/10.1080/00319100512331323977

Physics and Chemistry of Liquids
Vol. 43, No. 1, February 2005, 65–89

Taylor & Francis
Taylor & Francis Group

Influence of temperature on ultrasonic velocity measurements of ethanol + water + ethyl acetate mixtures

J.M. RESA†,*, C. GONZÁLEZ†, J.M. GOENAGA† and M. IGLESIAS‡

†Departamento de Ingeniería Química, Universidad del Pais Vasco,
Apto 450, Vitoria, España
‡Departament d'Enginyeria Química, Escola Tècnica Superior d'Enginyeria Química,
Universitat Rovira i Virgili,
Avinguda Països Catalans 26, Campus Sescelades, 43007 Tarragona, España

(Received 30 August 2004)

The ultrasonic velocity of the ternary mixtures ethanol + water + ethyl acetate at the range 288.15–323.15 K and atmospheric pressure, has been measured over the whole concentration range. The corresponding change of isentropic compressibility was computed from the experimental data. The results were fitted by means of a temperature-dependent equation, the parameters of which have been gathered in this experiment. The experimental ultrasonic velocities have been analyzed in terms of different theoretical models, an adequate agreement between the experimental and predicted values both in magnitude and sign being obtained, despite the high non-ideal trend of the studied mixture. The obtained experimental values indicate varying extent of interstitial accommodation among unlike molecules as a function of steric hindrance attending to ethyl acetate composition as key component and as a function of hydrogen bond and temperature attending to ethanol composition as key component.

Keywords: Ultrasonic velocities; Isentropic compressibilities; Derived magnitude; Estimation; Mixture; Ethanol; Water; Ethyl acetate; Temperature

1. Introduction

Knowledge of thermodynamic properties and phase equilibria of ethanol, water and the different flavour components in distilled alcoholic beverages is of practical interest to the food industry since industrial procedures applied are dependent on the temperature and pressure, in order to obtain a good quality final product. Nowadays, the use of

*Corresponding author. Fax: +34945013014. E-mail: iqpredij@vc.ehu.es

Physics and Chemistry of Liquids
ISSN 0031-9104 print: ISSN 1029-0451 online © 2005 Taylor & Francis Ltd
http://www.tandf.co.uk/journals
DOI: 10.1080/00319100512331323977

physical methods for mixture analysis yields better results than current chemical procedures for showing a higher accuracy and on-line application capability in the study of liquid phase characteristics and mixing phenomenae. Thermodynamic studies provide the additional advantage of an interesting trend of analysis of microscale interaction for understanding macroscale behaviour of gases and liquids on mixing. In accordance with this, a considerable amount of data has been developed in the field of thermodynamic properties, although a great scarcity of data is observed in open literature for mixtures present in commercial alcoholic beverages. Such properties are strongly dependent on the hydrogen-bond potency of hydroxyl groups, chain length, isomeric structures, and molecular package. Considering the different places of origin of grapes, thermal conditions of fermentation reactions and the complexity of composition and molecular chains of components, a considerable lack of accuracy or thermodynamic consistency can be observed in the disposable open literature data. In what is referred to as multicomponent mixtures, the scarcity of data references is greater, due to the relatively important non-ideality, as well as the complexity of a wide study and the time consuming nature of experimental procedures. It is not always possible to obtain proper values at such temperature and pressure, more so when mixtures in non-standard conditions are being referred to. Simulation and optimization are not used correctly in this matter, an overestimation of equipment or high energy-consuming conditions being usually applied due to inaccurate calculations. The difficulties of simulation in these types of processes have been commented upon previously [1]. As a continuation of previous works related to alcoholic beverage components [2,3], we present in this article the temperature dependence of the isentropic compressibilities of the mixture ethanol + water + ethyl acetate at the range 288.15–323.15 K and at atmospheric pressure, as a function of molar fraction. From the experimental values, the excess molar volumes were computed, a temperature-dependent Cibulka type polynomial being fitted to the results [3,4]. Due to the expense of the experimental measurement of such data, and current process design being strongly computer oriented, consideration was also given to how accurate theoretical models work. Despite the importance of computation in chemical processes, the theoretical procedures published in scientific journals are not very accurate and are of wide application. Our purpose is to discuss the dependence of the isentropic compressibility on mixing and other acoustic parameters on the composition and molecular structure, in order to provide a better understanding of the factors which contribute to the special behaviour on enclosing slight polar molecules into a hydroxylic environment, where the solvent is of shorter chain length and different molecular nature. Due to the importance of theoretical assumptions on industrial design, different procedures [5–9] were applied for the isentropic compressibilities, and the obtained results were analyzed and commented upon. We have attempted to explain the physico-chemical behaviour of the mixtures mentioned earlier, in order to explore the strength and nature of the interactions between the components by deriving various thermodynamic parameters from the ultrasonic velocity and density data [3]. The analysis of excess acoustic magnitudes pointed out the availability of intense effects among unlike molecules at a predetermined range of concentration (equimolar compositions). Attending to the deviation of computed data, we arrive at the conclusion that the application of the FLT model produces the results closest to theoretical calculations, despite the high non-ideal trend of mixtures.

2. Experimental

All chemical solvents used in the preparation of samples were of Merck quality with purity better than 99.5 mol%. The pure components were stored, protected from sun light, and kept under constant humidity and temperature conditions. In order to reduce fraction molar errors, the vapour space into the vessels was minimized during sample preparation. Mixtures were prepared by mass using a Salter ER-182A balance, the whole composition range of the ternary mixture being covered. The accuracy in molar fractions was obtained as higher than $\pm 5 \times 10^{-4}$. The ultrasonic velocities were measured with an Anton Paar DSA-48 device with a precision of $\pm 1\,\mathrm{m\,s^{-1}}$. Calibration of the apparatus was performed periodically, in accordance with technical specifications, using Millipore quality water (resistivity, 18.2 $\mathrm{M\Omega\,cm}$) and ambient air. Maximum deviation in the calculation of changes of isentropic compressibility for these mixtures has been estimated better than $1\ \mathrm{TPa^{-1}}$. The values of the pure components, as well as, open literature data are given in table 1. Further details about techniques and procedure in our laboratory can be obtained from previously published works [11].

3. Data procedure

3.1 *Correlation of derived magnitudes*

The changes of isentropic compressibilities are presented in table 2 and were computed from equation (1):

$$\delta Q = Q - \sum_{i=1}^{N} x_i Q_i \tag{1}$$

In this equation, δQ means the variation of a magnitude Q (κ_S, isentropic compressibilities calculated by the Laplace–Newton equation from density and ultrasonic velocity), Q_i is the pure solvent magnitude, x_i is the mole fraction, and N is the number of components into the mixtures. A Redlich–Kister [12] type equation was used to correlate the derived properties of the binary mixtures, by the unweighted least squares method, all experimental points weighting equally:

$$\delta Q_{ij} = x_i \cdot x_j \cdot \sum_{p=0}^{m} B_p \cdot (x_i - x_j)^p, \tag{2}$$

where δQ_{ij} stands for the derived magnitude, B_p are the fitting parameters and m is the degree of the polynomial, determined applying the F-test due to Bevington [13]. These binary parameters were collected from previous works [14,15]. The B_p parameters were computed using a non-linear optimization algorithm due to Marquardt [16]. The ternary derived magnitudes were fitted to the equation:

$$\delta Q_{123} = \delta Q_{12} + \delta Q_{13} + \delta Q_{23} + \Delta_{123} \tag{3}$$

where the binary magnitudes δQ_{ij} have been correlated to equation (2) and Δ_{123} is the ternary contribution fitted by means of a modified Cibulka equation [3,4]:

$$\Delta_{123} = x_1 x_2 x_3 RT \cdot (B_0 + B_1 x_1 + B_2 x_2) \tag{4}$$

Table 1. Comparison of experimental speed of sound ($m\,s^{-1}$) with literature data for chemicals at the studied temperatures.

Component	Molecular weight	288.15 K	290.65 K	293.15 K	295.65 K	298.15 K	300.65 K	303.15 K	305.65 K	308.15 K	310.65 K	313.15 K	315.65 K	318.15 K	320.65 K	323.15 K	lit. (298.15 K)
Ethanol	46.1	1178.2	1169.1	1160.3	1151.6	1143.1	1134.6	1126.2	1117.8	1109.4	1101	1092.7	1084.3	1075.9	1067.5	1058.8	1143[a]
Water	18.0	1466.4	1474.7	1482.5	1489.9	1496.9	1503.4	1509.5	1515.1	1520.3	1525.0	1529.3	1533.2	1536.6	1539.6	1542.1	1497[a]
Ethyl acetate	88.1	1183.6	1172.0	1160.5	1149.0	1137.7	1126.4	1115.3	1104.0	1093.0	1081.8	1070.7	1059.6	1048.5	1037.3	1026.2	1138[b]

[a] Alberto Arce, Alberto Arce Jr., Eva Rodil, Ana Soto, *J. Chem. Eng. Data*, **45**, 536–539 (2000).
[b] Nandhibatla V. Sastry, Mitesh, *J. Chem. Eng. Data*, **48**, 1019–1027 (2003).

Table 2. Ultrasonic velocities, isentropic compresibilities and change of isentropic compresibilities for ternary mixture at range of 288.15–323.15 K.

x_1	x_2	U/ (m × s^{-1})	κ_s / (TPa^{-1})	$\delta\kappa_s$/ (TPa^{-1})	x_1	x_2	u/ (m × s^{-1})	κ_s / (TPa^{-1})	$\delta\kappa_s$/ (TPa^{-1})
323.15 K									
0.8953	0.0546	1070.1	1123.6	0.0	0.2998	0.2026	1068.8	1031.9	48.4
0.0519	0.0601	1035.9	1081.2	18.4	0.3001	0.3002	1095.7	976.7	59.0
0.8040	0.0961	1076.9	1091.9	2.5	0.2994	0.3994	1130.0	912.6	61.9
0.6977	0.1003	1067.9	1091.1	11.7	0.2998	0.5008	1177.8	833.9	51.4
0.6985	0.2016	1110.6	1008.5	−2.7	0.2998	0.6004	1251.8	732.0	16.7
0.5974	0.3023	1141.1	939.2	2.8	0.1990	0.1058	1044.5	1074.8	32.9
0.5985	0.1035	1061.5	1088.5	18.0	0.1994	0.2048	1064.0	1030.4	55.1
0.4997	0.4002	1174.7	869.4	5.6	0.2006	0.2997	1086.1	983.4	72.1
0.5002	0.2980	1121.1	958.0	25.2	0.1989	0.4039	1113.8	928.0	87.0
0.4977	0.2043	1085.5	1024.4	28.6	0.1990	0.5007	1147.6	867.4	91.7
0.4957	0.1084	1055.5	1086.1	25.9	0.2001	0.5997	1199.3	786.2	77.2
0.3976	0.1078	1050.8	1083.4	29.3	0.1998	0.7007	1293.0	667.0	26.2
0.3989	0.2026	1075.6	1030.4	40.2	0.1016	0.2018	1059.8	1029.4	58.8
0.3930	0.3124	1110.9	960.5	44.7	0.1503	0.0502	1034.4	1094.0	17.8
0.3993	0.4017	1150.8	891.8	35.8	0.2483	0.0565	1036.1	1099.8	21.3
0.4008	0.4987	1210.7	801.3	10.7	0.1494	0.7978	1394.3	559.5	−12.5
0.2996	0.1006	1045.7	1083.1	30.8	0.2500	0.6987	1335.4	629.8	−15.8
320.65 K									
0.8953	0.0546	1078.7	1102.7	0.2	0.2998	0.2026	1078.9	1009.2	45.7
0.0519	0.0601	1047.0	1054.7	17.2	0.3001	0.3002	1105.7	955.9	55.5
0.8040	0.0961	1085.8	1070.9	1.9	0.2994	0.3994	1139.5	894.7	58.4
0.6977	0.1003	1077.4	1068.5	9.9	0.2998	0.5008	1186.9	818.7	47.8
0.6985	0.2016	1119.6	989.4	−3.8	0.2998	0.6004	1260.4	720.1	13.6
0.5974	0.3023	1150.1	922.0	1.2	0.1990	0.1058	1055.0	1049.9	31.2
0.5985	0.1035	1071.4	1065.0	15.7	0.1994	0.2048	1074.6	1006.9	52.1
0.4997	0.4002	1183.4	854.2	3.8	0.2006	0.2997	1096.0	962.5	68.9
0.5002	0.2980	1130.3	939.6	23.1	0.1989	0.4039	1123.6	909.1	83.0
0.4977	0.2043	1095.3	1002.9	26.0	0.1990	0.5007	1156.6	851.4	87.8
0.4957	0.1084	1065.5	1062.4	23.8	0.2001	0.5997	1207.9	772.8	73.1
0.3976	0.1078	1061.2	1058.7	26.8	0.1998	0.7007	1300.6	657.7	23.3
0.3989	0.2026	1085.4	1008.5	37.8	0.1016	0.2018	1070.4	1005.6	56.0
0.3930	0.3124	1120.6	940.8	41.4	0.1503	0.0502	1045.1	1068.1	17.0
0.3993	0.4017	1159.8	875.3	33.2	0.2483	0.0565	1046.8	1073.9	19.7
0.4008	0.4987	1219.3	787.8	8.3	0.1494	0.7978	1400.9	553.1	−14.9
0.2996	0.1006	1056.2	1058.1	28.7	0.2500	0.6987	1343.2	621.0	−18.4
318.15 K									
0.8953	0.0546	1087.5	1081.7	−0.5	0.2998	0.2026	1089.3	986.6	42.5
0.0519	0.0601	1058.0	1029.0	16.2	0.3001	0.3002	1115.6	935.9	52.2
0.8040	0.0961	1095.0	1049.8	0.4	0.2994	0.3994	1149.0	877.1	54.7
0.6977	0.1003	1086.9	1046.5	8.0	0.2998	0.5008	1195.8	804.1	44.3
0.6985	0.2016	1128.8	970.3	−5.6	0.2998	0.6004	1268.6	708.8	10.6
0.5974	0.3023	1159.1	904.9	−0.8	0.1990	0.1058	1065.6	1025.3	29.3
0.5985	0.1035	1081.2	1042.3	13.6	0.1994	0.2048	1084.9	984.2	49.3
0.4997	0.4002	1192.3	839.1	1.5	0.2006	0.2997	1106.7	940.8	64.5
0.5002	0.2980	1139.7	921.2	20.4	0.1989	0.4039	1133.1	890.9	79.1
0.4977	0.2043	1105.0	981.9	23.4	0.1990	0.5007	1165.6	835.6	83.6
0.4957	0.1084	1075.4	1039.2	21.5	0.2001	0.5997	1216.5	759.8	69.0
0.3976	0.1078	1071.4	1035.0	24.6	0.1998	0.7007	1308.3	648.3	19.9
0.3989	0.2026	1095.5	986.6	34.7	0.1016	0.2018	1081.1	982.4	53.3
0.3930	0.3124	1130.3	921.8	38.2	0.1503	0.0502	1056.0	1042.3	15.6
0.3993	0.4017	1169.2	858.7	29.9	0.2483	0.0565	1057.5	1048.3	17.9
0.4008	0.4987	1228.0	774.5	5.5	0.1494	0.7978	1407.5	546.6	−17.8
0.2996	0.1006	1066.7	1033.6	26.4	0.2500	0.6987	1350.8	612.5	−21.0

(*continued*)

Table 2. Continued.

x_1	x_2	U/ (m × s^{-1})	κ_s / (TPa^{-1})	$\delta\kappa_s$/ (TPa^{-1})	x_1	x_2	u/ (m × s^{-1})	κ_s / (TPa^{-1})	$\delta\kappa_s$/ (TPa^{-1})
315.65 K									
0.8953	0.0546	1096.2	1061.6	−1.0	0.2998	0.2026	1099.5	965.2	39.5
0.0519	0.0601	1069.1	1004.3	15.0	0.3001	0.3002	1125.5	916.6	48.6
0.8040	0.0961	1104.0	1029.7	−0.9	0.2994	0.3994	1158.4	860.3	51.0
0.6977	0.1003	1096.4	1025.3	6.1	0.2998	0.5008	1204.9	789.7	40.5
0.6985	0.2016	1137.9	952.1	−7.3	0.2998	0.6004	1276.7	698.0	7.6
0.5974	0.3023	1168.0	888.6	−2.8	0.1990	0.1058	1076.2	1001.8	27.3
0.5985	0.1035	1091.0	1020.5	11.4	0.1994	0.2048	1095.3	962.4	46.4
0.4997	0.4002	1201.3	824.2	−1.2	0.2006	0.2997	1116.7	921.0	61.0
0.5002	0.2980	1149.2	903.3	17.4	0.1989	0.4039	1142.7	873.3	75.0
0.4977	0.2043	1114.8	961.8	20.7	0.1990	0.5007	1174.7	820.2	79.3
0.4957	0.1084	1085.6	1016.6	19.0	0.2001	0.5997	1224.8	747.4	64.9
0.3976	0.1078	1081.6	1012.1	22.3	0.1998	0.7007	1315.7	639.4	16.6
0.3989	0.2026	1105.5	965.7	31.9	0.1016	0.2018	1091.5	960.4	50.8
0.3930	0.3124	1139.9	903.5	35.0	0.1503	0.0502	1066.9	1017.5	14.2
0.3993	0.4017	1178.4	842.7	26.6	0.2483	0.0565	1068.1	1024.1	16.3
0.4008	0.4987	1236.7	761.5	2.6	0.1494	0.7978	1414.1	540.3	−20.8
0.2996	0.1006	1077.1	1010.3	24.3	0.2500	0.6987	1358.4	604.3	−23.9
313.15 K									
0.8953	0.0546	1104.9	1041.9	−1.7	0.2998	0.2026	1109.7	944.3	36.6
0.0519	0.0601	1079.9	980.7	14.2	0.3001	0.3002	1135.3	897.8	45.2
0.8040	0.0961	1113.0	1010.1	−2.1	0.2994	0.3994	1167.8	843.8	47.3
0.6977	0.1003	1105.7	1005.0	4.5	0.2998	0.5008	1213.6	776.1	36.9
0.6985	0.2016	1146.8	934.6	−8.8	0.2998	0.6004	1284.7	687.4	4.4
0.5974	0.3023	1177.0	872.4	−5.1	0.1990	0.1058	1086.9	978.8	25.2
0.5985	0.1035	1100.6	999.5	9.5	0.1994	0.2048	1105.5	941.5	43.8
0.4997	0.4002	1209.9	810.1	−3.6	0.2006	0.2997	1126.7	901.7	57.5
0.5002	0.2980	1158.5	886.0	14.6	0.1989	0.4039	1152.1	856.3	71.1
0.4977	0.2043	1124.4	942.3	18.2	0.1990	0.5007	1183.8	805.3	74.8
0.4957	0.1084	1095.4	995.2	17.0	0.2001	0.5997	1233.1	735.4	60.7
0.3976	0.1078	1091.8	989.9	20.0	0.1998	0.7007	1323.3	630.4	12.9
0.3989	0.2026	1115.4	945.6	29.1	0.1016	0.2018	1102.0	939.0	48.2
0.3930	0.3124	1149.5	885.7	31.8	0.1503	0.0502	1077.7	993.8	13.0
0.3993	0.4017	1187.6	827.3	23.3	0.2483	0.0565	1078.7	1000.5	14.7
0.4008	0.4987	1245.1	749.1	−0.2	0.1494	0.7978	1420.3	534.5	−23.8
0.2996	0.1006	1087.5	987.6	22.3	0.2500	0.6987	1365.5	596.5	−26.6
310.65 K									
0.8953	0.0546	1113.7	1022.8	−2.5	0.2998	0.2026	1119.7	924.3	33.8
0.0519	0.0601	1090.8	957.8	13.3	0.3001	0.3002	1145.1	879.7	41.8
0.8040	0.0961	1121.8	991.3	−3.2	0.2994	0.3994	1177.2	827.8	43.4
0.6977	0.1003	1115.1	985.1	2.7	0.2998	0.5008	1222.4	762.8	33.1
0.6985	0.2016	1155.7	917.5	−10.4	0.2998	0.6004	1292.7	677.1	1.0
0.5974	0.3023	1185.8	857.0	−7.3	0.1990	0.1058	1097.3	956.8	23.4
0.5985	0.1035	1110.3	979.0	7.4	0.1994	0.2048	1115.8	920.9	40.8
0.4997	0.4002	1218.6	796.4	−6.1	0.2006	0.2997	1136.6	883.1	54.0
0.5002	0.2980	1167.8	869.4	11.8	0.1989	0.4039	1161.6	839.7	66.9
0.4977	0.2043	1134.0	923.5	15.6	0.1990	0.5007	1192.5	791.2	70.7
0.4957	0.1084	1105.3	974.0	14.7	0.2001	0.5997	1241.2	723.7	56.5
0.3976	0.1078	1102.0	968.5	17.8	0.1998	0.7007	1330.5	622.0	9.3
0.3989	0.2026	1125.2	926.0	26.3	0.1016	0.2018	1112.4	918.3	45.6
0.3930	0.3124	1159.0	868.4	28.4	0.1503	0.0502	1088.3	971.0	12.1
0.3993	0.4017	1196.5	812.5	20.1	0.2483	0.0565	1089.2	977.9	13.3
0.4008	0.4987	1253.5	737.1	−3.1	0.1494	0.7978	1426.5	528.6	−27.1
0.2996	0.1006	1097.8	965.8	20.3	0.2500	0.6987	1372.8	588.7	−29.8
308.15 K									
0.8953	0.0546	1122.3	1004.3	−3.0	0.2998	0.2026	1129.9	904.8	31.0
0.0519	0.0601	1101.8	935.5	12.5	0.3001	0.3002	1154.9	862.0	38.4

(*continued*)

Table 2. Continued.

x_1	x_2	U/ (m × s^{-1})	κ_s / (TPa^{-1})	$\delta\kappa_s$/ (TPa^{-1})	x_1	x_2	u/ (m × s^{-1})	κ_s / (TPa^{-1})	$\delta\kappa_s$/ (TPa^{-1})
0.8040	0.0961	1130.8	972.7	−4.4	0.2994	0.3994	1186.6	812.3	39.7
0.6977	0.1003	1124.5	965.7	1.0	0.2998	0.5008	1231.2	749.7	29.1
0.6985	0.2016	1164.7	900.8	−11.9	0.2998	0.6004	1300.7	667.0	−2.4
0.5974	0.3023	1194.7	841.9	−9.4	0.1990	0.1058	1107.9	935.4	21.7
0.5985	0.1035	1120.0	959.0	5.5	0.1994	0.2048	1126.1	901.2	38.2
0.4997	0.4002	1227.3	782.9	−8.7	0.2006	0.2997	1146.5	865.0	50.7
0.5002	0.2980	1177.1	853.1	9.0	0.1989	0.4039	1171.1	823.5	62.9
0.4977	0.2043	1143.7	905.1	13.2	0.1990	0.5007	1201.2	777.3	66.4
0.4957	0.1084	1115.2	953.7	12.7	0.2001	0.5997	1249.3	712.4	52.2
0.3976	0.1078	1112.2	947.6	15.7	0.1998	0.7007	1337.8	613.8	5.5
0.3989	0.2026	1135.2	906.8	23.5	0.1016	0.2018	1122.8	898.3	43.2
0.3930	0.3124	1168.7	851.5	25.1	0.1503	0.0502	1099.1	948.7	11.1
0.3993	0.4017	1205.7	797.9	16.8	0.2483	0.0565	1099.8	955.9	12.1
0.4008	0.4987	1261.9	725.3	−6.1	0.1494	0.7978	1432.6	523.0	−30.5
0.2996	0.1006	1108.2	944.5	18.4	0.2500	0.6987	1380.1	581.1	−33.0
305.65 K									
0.8953	0.0546	1131.0	986.3	−3.5	0.2998	0.2026	1140.0	885.8	28.1
0.0519	0.0601	1112.7	914.1	11.4	0.3001	0.3002	1164.7	844.9	34.8
0.8040	0.0961	1139.7	954.7	−5.6	0.2994	0.3994	1195.9	797.3	35.8
0.6977	0.1003	1133.8	947.0	−0.6	0.2998	0.5008	1239.9	737.2	25.3
0.6985	0.2016	1173.6	884.6	−13.6	0.2998	0.6004	1308.6	657.3	−6.0
0.5974	0.3023	1203.6	827.0	−11.8	0.1990	0.1058	1118.5	914.6	19.6
0.5985	0.1035	1129.6	939.7	3.6	0.1994	0.2048	1136.4	881.9	35.3
0.4997	0.4002	1236.0	769.8	−11.4	0.2006	0.2997	1156.5	847.4	47.1
0.5002	0.2980	1186.3	837.3	6.1	0.1989	0.4039	1180.4	808.1	58.8
0.4977	0.2043	1153.4	887.2	10.4	0.1990	0.5007	1210.0	763.9	62.0
0.4957	0.1084	1125.2	933.8	10.4	0.2001	0.5997	1257.3	701.4	47.8
0.3976	0.1078	1122.3	927.5	13.6	0.1998	0.7007	1345.0	605.8	1.6
0.3989	0.2026	1145.1	888.3	20.7	0.1016	0.2018	1133.3	878.8	40.5
0.3930	0.3124	1178.1	835.3	21.9	0.1503	0.0502	1109.8	927.2	9.9
0.3993	0.4017	1214.7	783.8	13.4	0.2483	0.0565	1110.4	934.6	10.5
0.4008	0.4987	1270.3	713.8	−9.3	0.1494	0.7978	1438.6	517.5	−34.2
0.2996	0.1006	1118.5	924.0	16.4	0.2500	0.6987	1387.2	573.8	−36.5
303.15 K									
0.8953	0.0546	1139.7	968.6	−3.9	0.2998	0.2026	1150.2	867.4	25.3
0.0519	0.0601	1123.8	893.1	10.5	0.3001	0.3002	1174.6	828.1	31.4
0.8040	0.0961	1148.7	937.1	−6.7	0.2994	0.3994	1205.2	782.6	31.9
0.6977	0.1003	1143.2	928.6	−2.2	0.2998	0.5008	1248.6	724.9	21.3
0.6985	0.2016	1182.6	868.6	−15.2	0.2998	0.6004	1316.5	647.7	−9.7
0.5974	0.3023	1212.5	812.6	−14.0	0.1990	0.1058	1129.1	894.5	18.0
0.5985	0.1035	1139.3	920.9	1.8	0.1994	0.2048	1146.8	863.1	32.5
0.4997	0.4002	1244.6	757.0	−14.1	0.2006	0.2997	1166.5	830.2	43.5
0.5002	0.2980	1195.6	821.9	3.3	0.1989	0.4039	1189.8	792.8	54.7
0.4977	0.2043	1163.0	869.8	8.1	0.1990	0.5007	1218.7	750.8	57.5
0.4957	0.1084	1135.2	914.4	8.3	0.2001	0.5997	1265.4	690.6	43.2
0.3976	0.1078	1132.5	907.9	11.7	0.1998	0.7007	1352.1	597.9	−2.6
0.3989	0.2026	1155.1	870.3	18.0	0.1016	0.2018	1143.7	859.9	38.0
0.3930	0.3124	1187.7	819.4	18.6	0.1503	0.0502	1120.7	906.3	8.9
0.3993	0.4017	1223.8	769.9	10.0	0.2483	0.0565	1121.0	913.8	9.2
0.4008	0.4987	1278.6	702.6	−12.4	0.1494	0.7978	1444.6	512.2	−38.0
0.2996	0.1006	1129.0	903.9	14.6	0.2500	0.6987	1394.3	566.6	−40.0
300.65 K									
0.8953	0.0546	1148.4	951.4	−4.5	0.2998	0.2026	1160.3	849.6	22.5
0.0519	0.0601	1134.7	872.9	9.6	0.3001	0.3002	1184.3	812.0	27.8
0.8040	0.0961	1157.7	920.0	−7.9	0.2994	0.3994	1214.5	768.3	27.9
0.6977	0.1003	1152.5	910.9	−3.8	0.2998	0.5008	1257.2	713.0	17.2

(*continued*)

Table 2. Continued.

x_1	x_2	U/ (m × s^{-1})	κ_s / (TPa^{-1})	$\delta\kappa_s$/ (TPa^{-1})	x_1	x_2	u/ (m × s^{-1})	κ_s / (TPa^{-1})	$\delta\kappa_s$/ (TPa^{-1})
0.6985	0.2016	1191.5	853.3	−16.8	0.2998	0.6004	1324.3	638.5	−13.5
0.5974	0.3023	1221.3	798.7	−16.3	0.1990	0.1058	1139.6	875.1	16.2
0.5985	0.1035	1148.9	902.7	0.1	0.1994	0.2048	1157.1	845.1	29.7
0.4997	0.4002	1253.2	744.5	−17.0	0.2006	0.2997	1176.5	813.6	39.8
0.5002	0.2980	1204.9	807.0	0.4	0.1989	0.4039	1199.1	778.2	50.5
0.4977	0.2043	1172.6	853.1	5.5	0.1990	0.5007	1227.4	738.0	52.9
0.4957	0.1084	1145.1	895.8	6.3	0.2001	0.5997	1273.3	680.2	38.5
0.3976	0.1078	1142.7	888.8	9.6	0.1998	0.7007	1359.2	590.3	−6.8
0.3989	0.2026	1165.0	852.9	15.2	0.1016	0.2018	1154.1	841.7	35.4
0.3930	0.3124	1197.2	803.9	15.2	0.1503	0.0502	1131.4	886.1	7.9
0.3993	0.4017	1232.7	756.6	6.5	0.2483	0.0565	1131.5	893.8	7.9
0.4008	0.4987	1286.9	691.7	−15.8	0.1494	0.7978	1450.3	507.1	−42.0
0.2996	0.1006	1139.3	884.7	12.7	0.2500	0.6987	1401.3	559.7	−43.7
298.15 K									
0.8953	0.0546	1157.2	934.5	−5.1	0.2998	0.2026	1170.5	832.2	19.7
0.0519	0.0601	1145.7	853.3	8.8	0.3001	0.3002	1194.2	796.1	24.3
0.8040	0.0961	1166.7	903.2	−9.0	0.2994	0.3994	1223.9	754.4	23.9
0.6977	0.1003	1161.9	893.5	−5.3	0.2998	0.5008	1265.9	701.3	12.9
0.6985	0.2016	1200.5	838.2	−18.6	0.2998	0.6004	1332.2	629.4	−17.5
0.5974	0.3023	1230.1	785.1	−18.6	0.1990	0.1058	1150.2	856.2	14.6
0.5985	0.1035	1158.6	885.0	−1.6	0.1994	0.2048	1167.4	827.4	26.9
0.4997	0.4002	1261.9	732.3	−19.9	0.2006	0.2997	1186.5	797.3	36.2
0.5002	0.2980	1214.1	792.4	−2.4	0.1989	0.4039	1208.5	763.8	46.2
0.4977	0.2043	1182.2	836.6	3.1	0.1990	0.5007	1236.1	725.6	48.3
0.4957	0.1084	1155.1	877.6	4.4	0.2001	0.5997	1281.3	670.0	33.8
0.3976	0.1078	1152.8	870.4	7.8	0.1998	0.7007	1366.2	582.9	−11.3
0.3989	0.2026	1174.9	835.9	12.5	0.1016	0.2018	1164.6	823.9	32.9
0.3930	0.3124	1206.7	788.9	11.8	0.1503	0.0502	1142.3	866.3	6.8
0.3993	0.4017	1241.8	743.4	2.9	0.2483	0.0565	1142.2	874.2	6.6
0.4008	0.4987	1295.2	681.1	−19.3	0.1494	0.7978	1456.0	502.0	−46.2
0.2996	0.1006	1149.8	866.4	11.5	0.2500	0.6987	1408.2	552.9	−47.6
295.65 K									
0.8953	0.0546	1166.0	917.9	−5.6	0.2998	0.2026	1180.8	815.2	16.9
0.0519	0.0601	1156.9	834.1	7.7	0.3001	0.3002	1204.1	780.7	20.7
0.8040	0.0961	1175.7	886.8	−10.2	0.2994	0.3994	1233.3	740.8	19.7
0.6977	0.1003	1171.4	876.5	−6.8	0.2998	0.5008	1274.6	689.8	8.6
0.6985	0.2016	1209.5	823.4	−20.3	0.2998	0.6004	1340.0	620.5	−21.7
0.5974	0.3023	1239.1	771.7	−21.1	0.1990	0.1058	1160.9	837.8	12.8
0.5985	0.1035	1168.3	867.7	−3.2	0.1994	0.2048	1177.9	810.2	24.1
0.4997	0.4002	1270.6	720.4	−22.9	0.2006	0.2997	1196.6	781.5	32.5
0.5002	0.2980	1223.5	778.0	−5.5	0.1989	0.4039	1218.0	749.7	41.8
0.4977	0.2043	1192.0	820.5	0.5	0.1990	0.5007	1244.8	713.4	43.5
0.4957	0.1084	1165.3	859.7	2.3	0.2001	0.5997	1289.1	660.1	28.8
0.3976	0.1078	1163.1	852.4	5.9	0.1998	0.7007	1373.1	575.6	−15.9
0.3989	0.2026	1184.9	819.2	9.7	0.1016	0.2018	1175.1	806.5	30.2
0.3930	0.3124	1216.4	774.1	8.3	0.1503	0.0502	1153.2	847.2	5.9
0.3993	0.4017	1250.9	730.5	−0.9	0.2483	0.0565	1152.9	855.2	5.4
0.4008	0.4987	1303.5	670.6	−22.9	0.1494	0.7978	1461.7	497.1	−50.6
0.2996	0.1006	1160.3	848.0	9.6	0.2500	0.6987	1415.2	546.2	−51.8
293.15 K									
0.8953	0.0546	1175.0	901.6	−6.1	0.2998	0.2026	1191.1	798.5	14.0
0.0519	0.0601	1168.1	815.4	7.0	0.3001	0.3002	1214.1	765.5	17.0
0.8040	0.0961	1185.0	870.6	−11.4	0.2994	0.3994	1242.8	727.3	15.5
0.6977	0.1003	1181.0	859.8	−8.4	0.2998	0.5008	1283.6	678.4	3.9
0.6985	0.2016	1218.7	808.7	−22.1	0.2998	0.6004	1348.0	611.6	−26.2
0.5974	0.3023	1248.1	758.4	−23.6	0.1990	0.1058	1171.7	819.7	11.2

(*continued*)

Table 2. Continued.

x_1	x_2	U/ (m × s^{-1})	κ_s / (TPa^{-1})	$\delta\kappa$s/ (TPa^{-1})	x_1	x_2	u/ (m × s^{-1})	κ_s / (TPa^{-1})	$\delta\kappa_s$/ (TPa^{-1})
0.5985	0.1035	1178.0	850.8	−4.6	0.1994	0.2048	1188.4	793.4	21.3
0.4997	0.4002	1279.5	708.5	−26.2	0.2006	0.2997	1206.8	765.9	28.7
0.5002	0.2980	1233.1	763.8	−8.6	0.1989	0.4039	1227.5	735.9	37.3
0.4977	0.2043	1201.8	804.7	−1.9	0.1990	0.5007	1253.6	701.5	38.6
0.4957	0.1084	1175.6	842.0	0.2	0.2001	0.5997	1297.1	650.2	23.7
0.3976	0.1078	1173.3	835.0	4.3	0.1998	0.7007	1380.2	568.4	−20.8
0.3989	0.2026	1195.1	802.9	7.0	0.1016	0.2018	1185.7	789.5	27.6
0.3930	0.3124	1226.2	759.5	4.8	0.1503	0.0502	1164.2	828.5	5.0
0.3993	0.4017	1260.2	717.8	−4.7	0.2483	0.0565	1163.8	836.4	4.1
0.4008	0.4987	1312.0	660.2	−26.7	0.1494	0.7978	1467.4	492.2	−55.4
0.2996	0.1006	1171.0	829.9	7.8	0.2500	0.6987	1422.3	539.5	−56.3
290.65 K									
0.8953	0.0546	1184.1	885.6	−6.7	0.2998	0.2026	1201.6	782.2	11.2
0.0519	0.0601	1179.3	797.3	6.2	0.3001	0.3002	1224.2	750.7	13.3
0.8040	0.0961	1194.3	854.7	−12.5	0.2994	0.3994	1252.3	714.2	11.2
0.6977	0.1003	1190.7	843.4	−9.8	0.2998	0.5008	1292.3	667.4	−0.7
0.6985	0.2016	1228.0	794.4	−24.0	0.2998	0.6004	1356.0	602.9	−30.9
0.5974	0.3023	1257.2	745.4	−26.2	0.1990	0.1058	1182.6	802.0	9.4
0.5985	0.1035	1187.4	834.9	−5.6	0.1994	0.2048	1199.0	776.8	18.4
0.4997	0.4002	1288.4	696.8	−29.5	0.2006	0.2997	1217.0	750.8	24.9
0.5002	0.2980	1242.6	750.0	−11.7	0.1989	0.4039	1237.1	722.5	32.8
0.4977	0.2043	1211.6	789.3	−4.4	0.1990	0.5007	1262.5	689.7	33.5
0.4957	0.1084	1186.0	824.8	−1.8	0.2001	0.5997	1305.0	640.8	18.5
0.3976	0.1078	1183.6	817.8	2.5	0.1998	0.7007	1387.2	561.4	−25.9
0.3989	0.2026	1205.3	786.9	4.2	0.1016	0.2018	1196.4	773.0	25.0
0.3930	0.3124	1236.0	745.4	1.3	0.1503	0.0502	1175.3	810.2	4.1
0.3993	0.4017	1269.4	705.4	−8.6	0.2483	0.0565	1174.6	818.5	3.0
0.4008	0.4987	1320.6	650.0	−30.7	0.1494	0.7978	1473.1	487.5	−60.4
0.2996	0.1006	1181.6	812.3	6.1	0.2500	0.6987	1429.4	532.9	−61.0
288.15 K									
0.8953	0.0546	1193.1	869.2	−7.6	0.2998	0.2026	1212.0	765.8	7.8
0.0519	0.0601	1190.2	779.6	5.3	0.3001	0.3002	1234.0	735.9	9.4
0.8040	0.0961	1203.6	838.4	−14.0	0.2994	0.3994	1261.9	700.9	6.3
0.6977	0.1003	1199.9	827.4	−11.0	0.2998	0.5008	1300.9	656.3	−5.6
0.6985	0.2016	1237.2	779.6	−26.3	0.2998	0.6004	1363.5	594.4	−35.5
0.5974	0.3023	1266.3	732.1	−29.3	0.1990	0.1058	1193.4	784.4	7.2
0.5985	0.1035	1197.1	818.3	−7.3	0.1994	0.2048	1209.5	760.5	15.2
0.4997	0.4002	1297.2	685.0	−33.2	0.2006	0.2997	1227.3	735.4	20.5
0.5002	0.2980	1252.2	735.8	−15.4	0.1989	0.4039	1246.3	709.1	28.0
0.4977	0.2043	1221.3	773.9	−7.1	0.1990	0.5007	1271.2	677.9	27.9
0.4957	0.1084	1196.4	807.4	−4.3	0.2001	0.5997	1312.8	631.1	12.8
0.3976	0.1078	1194.0	800.6	0.4	0.1998	0.7007	1394.3	554.0	−31.7
0.3989	0.2026	1215.6	770.6	0.7	0.1016	0.2018	1206.9	756.6	22.0
0.3930	0.3124	1245.6	731.1	−2.7	0.1503	0.0502	1186.3	792.0	2.7
0.3993	0.4017	1278.7	692.7	−13.1	0.2483	0.0565	1185.3	800.5	1.7
0.4008	0.4987	1329.0	639.6	−35.1	0.1494	0.7978	1478.6	482.5	−65.9
0.2996	0.1006	1192.1	794.9	4.1	0.2500	0.6987	1436.0	526.5	−65.9

where x_i is the molar fraction, R, the universal constant for gases and T, the temperature in Kelvin. The B_i parameters are temperature dependent as follows:

$$B_i = \sum_{j=0}^{3} B_{ij} \cdot T^j \tag{5}$$

The B_{ij} parameters were computed and enclosed with their root mean square deviations in table 3. The root mean square deviations presented were computed

Table 3. Parameters of equation (5) in the range 288.15–323.15 K and σ in accordance to equation (6).

$C_{00} = -538628.016$	$C_{01} = 5562.714$	$C_{02} = -19.161$	$C_{03} = 0.022$	
$C_{10} = 780908.570$	$C_{11} = -8007.174$	$C_{12} = 27.342$	$C_{13} = -0.031$	
$C_{20} = 368671.033$	$C_{21} = -4406.590$	$C_{22} = 16.795$	$C_{23} = -0.021$	$\sigma = 17.65$

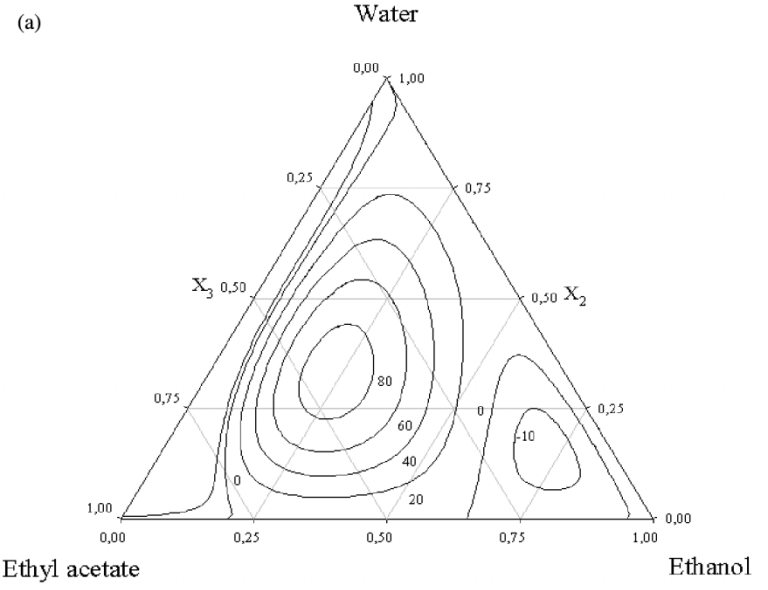

Figure 1. Curves of changes of isentropic compressibility for ethanol + water + ethyl acetate (a) 323.15 K; (b) 298.15 K; (c) 288.15 K.

using the equation (6), where z is the value of the derived magnitude, and n_{DAT} is the number of experimental data:

$$\sigma = \left(\frac{\sum_{i=1}^{n_{DAT}} (z_{exp} - z_{pred})^2}{n_{DAT}} \right)^{1/2} \quad (6)$$

No previously published data have been found at the studied conditions for this ternary mixture. Curves of constant changes of isentropic compressibility for the ternary mixture ethanol + water + ethyl acetate, have been plotted in figures 1(a), (b) and (c), at the extreme values of temperature and standard conditions. In these figures, a clear negative tendency is shown for this mixture at the vicinity of ethanol + water mixture. This trend is diminished towards rising ethyl acetate compositions. Such an effect is reflected in terms of derived value as two different regions in what to the sign is referred, first a negative zone near ethanol but increasing around diluted acetate compositions as well as temperature rises. Second, a positive region exists with a maximum at almost equimolar compositions, which is increased for rising temperatures (figures 1(a), (b) and (c)). It is worthwhile to point out the huge ternary contribution in either the positive or the negative zone (figures 2(a), (b) and (c)). As an example, it is possible to compare the values of the change of isentropic compressibility and the corresponding ternary contribution at the same temperature and observe that the

(b)

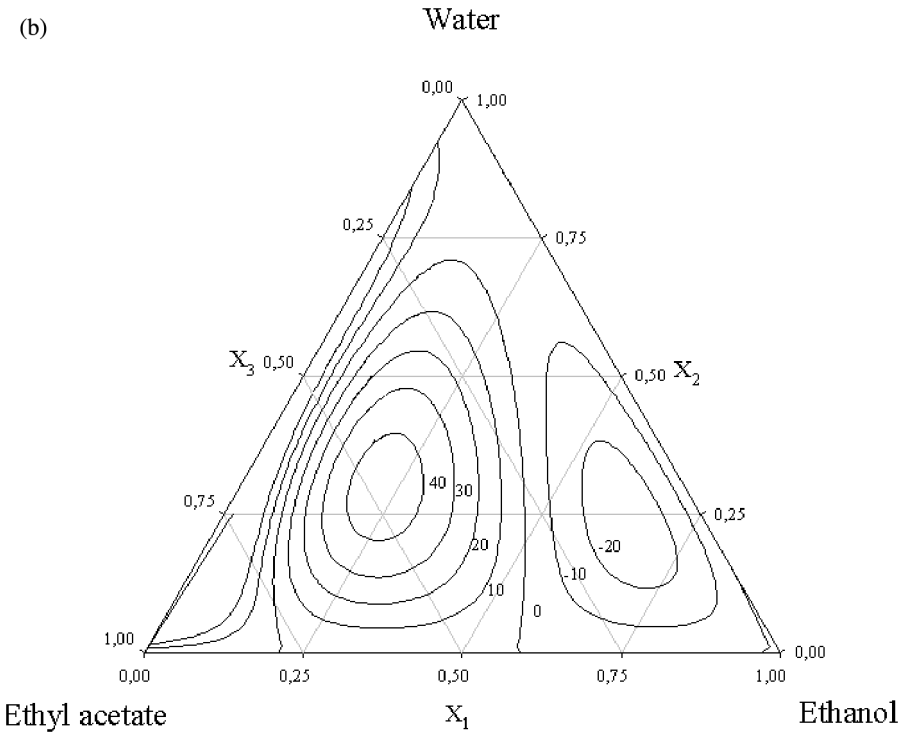

(c)

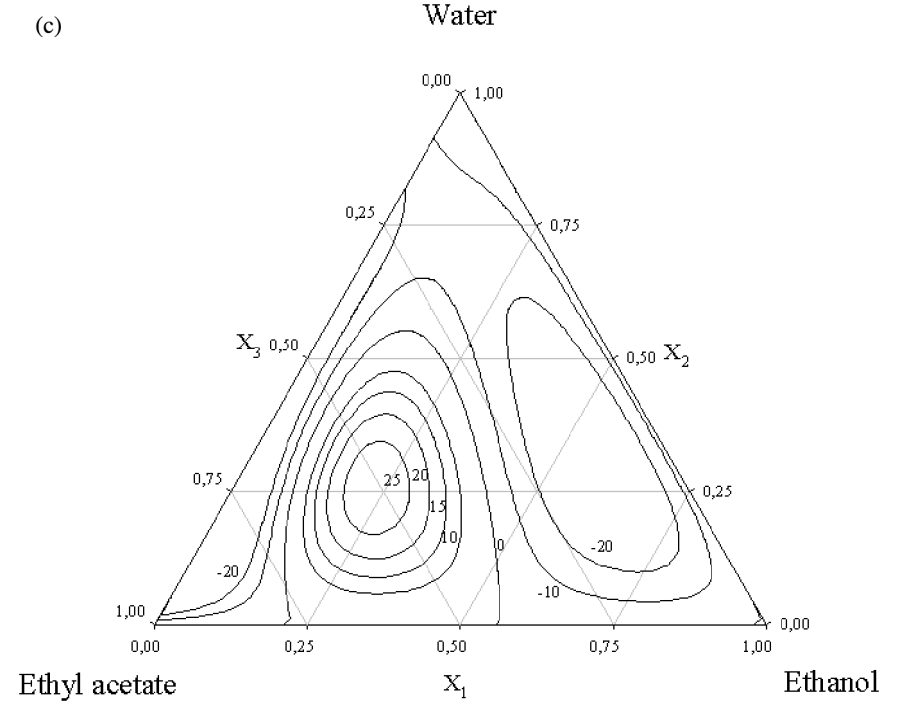

Figure 1. Continued

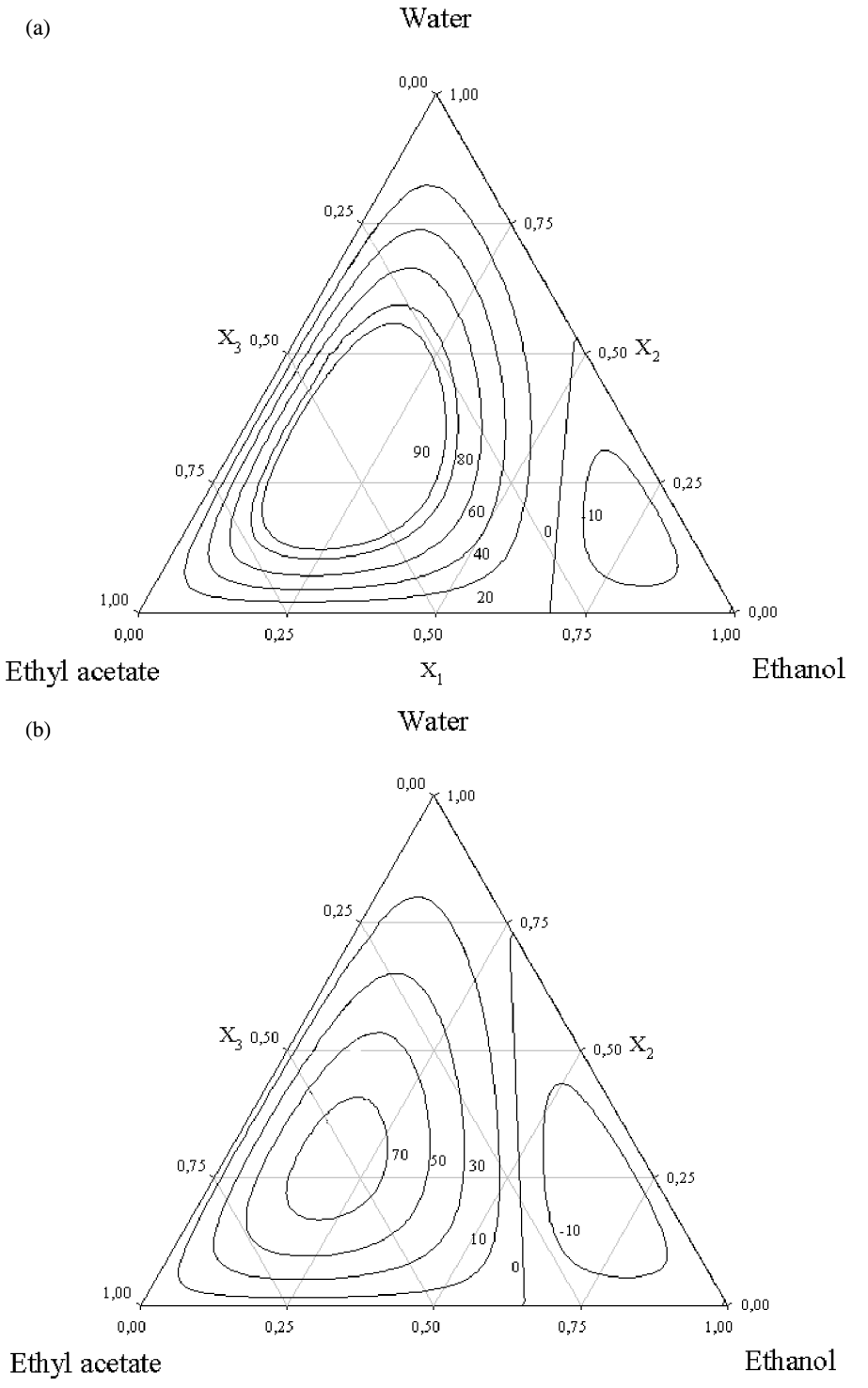

Figure 2. Curves of ternary contribution of the changes of isentropic compressibility for ethanol + water + ethyl acetate: (a) 323.15 K; (b) 298.15 K; (c) 288.15 K.

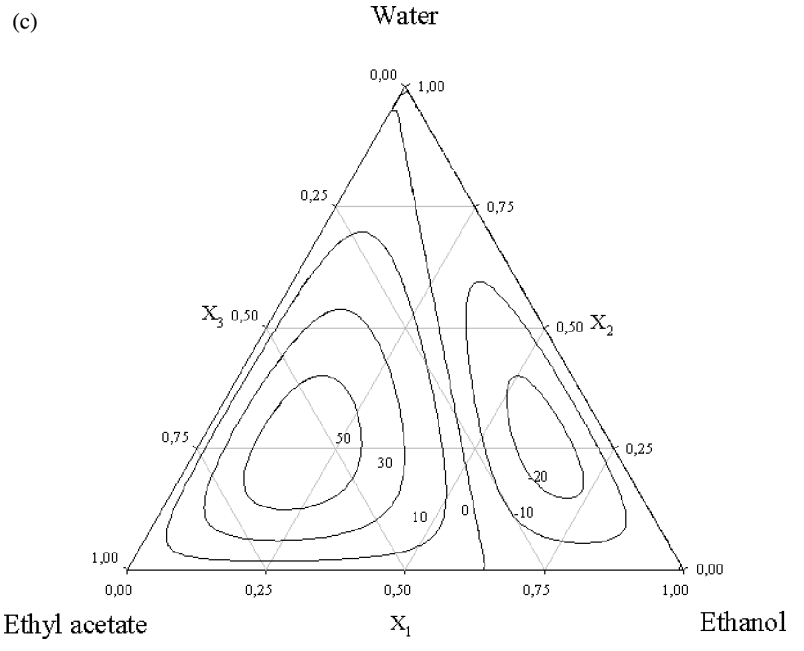

Figure 2. Continued.

latter decides the final value and sign of the derived magnitude. Ternary interactions are then very important to quantify the nonideality of the magnitude and point out the role of each component of the diluted mixtures, as for alcoholic beverages, where the presence of ethyl acetate is in terms of high dilution.

3.2 *Acoustic parameters*

We have attempted to explain the physico-chemical behaviour of the mixtures indicated above, in order to explore the strength and nature of the interactions between the components by deriving various thermodynamic parameters from the ultrasonic velocity and density data. The parameters derived from the experimental measured data were intermolecular free length (L_f), the van der Waals' constant (b), molecular radius (r), geometrical volume (B), molar surface area (Y), available volume (V_a), volume at absolute zero (V_0), molar sound velocity (R), collision factor (S), specific acoustic impedance (Z), relative association (R_A), and molecular association (M_A), attending to the following set of equations:

$$L_f = \left(\frac{K}{u \cdot \rho^{1/2}}\right) \tag{6}$$

$$b = \left(\frac{M}{\rho}\right) - \left(\frac{RT}{\rho \cdot u^2}\right) \cdot \left(\left[1 + \frac{M \cdot u^2}{3RT}\right]^{1/2} - 1\right) \tag{7}$$

$$r = \left(\frac{3b}{16\pi N}\right)^{1/3} \tag{8}$$

$$B = \frac{4}{3}\pi r^3 N \tag{9}$$

$$Y = (36\pi N B^2)^{1/3} \tag{10}$$

$$V_a = V\left(1 - \left(\frac{u}{u_\infty}\right)\right) \tag{11}$$

$$V_0 = V - V_a \tag{12}$$

$$R = \frac{M \cdot u^{1/3}}{\rho} \tag{13}$$

$$S = \frac{u \cdot V}{B \cdot u_\infty} \tag{14}$$

$$Z = u \cdot \rho \tag{15}$$

$$R_A = \left(\frac{\rho_{mix}}{\rho}\right) \cdot \left(\frac{u}{u_{mix}}\right)^{1/3} \tag{16}$$

$$M_A = \left[\left(\frac{u_{mix}}{\sum_i x_i u_i}\right)^2 - 1\right] \tag{17}$$

where L_f is the free length of ideal mixing, K is a temperature-dependent constant ($K = (93.875 + 0.375\,T) \times 10^{-8}$, u_∞ is taken as $1600\,\mathrm{ms}^{-1}$ [9], and R and π are common universal constants. These parameters are compiled in table 4 for the pure compounds. The variation in the magnitudes L_f and Z (by means of equation (1) for the ternary mixtures are shown in figures 3 and 4 respectively, showing these magnitudes as a function of $z = \pi_{i=1}^{N} x_i$, where x_i stands for the same meaning as indicated above. These figures led to different pseudobinary (low values of z) and ternary composition (high values of z) trends. In accordance with the contractive trend observed for other ternary mixtures which are being studied in our laboratory, extreme values are gathered at pseudobinary concentrations, which reinforce the supposition of the strong disturbance in the accomodation of hydroxylic molecules by the aliphatic end of ethyl acetate.

The compressibility solvation numbers are calculated using the following equation, according to the usual expressions [10]:

$$n_S = \left(\frac{n_{solvent}}{n_{solute}}\right) \cdot \left(1 - \frac{\kappa_S}{\kappa_{So}}\right) \tag{18}$$

where $n_{solvent}$ and n_{solute} are mol number of solvent and solute, respectively. The equation used for computing the compressibility solvation numbers assumes that the hydration layer around the ethanol molecule is incompressible, which is not the case; despite this, it provides an acceptable approximation of the extent of interaction of ethanol with water. These parameters are derived from isentropic compressibility measurements and therefore account for the first two layers of water around the solute. Falling compressibility hydration numbers indicate that a smaller number of molecules

Table 4. Acoustic parameters for the pure compounds enclosed into the studied mixtures.

	L_f (Å)	b ($m^3\,mol^{-1}$)	$r \times 10^{12}$ (m)	B ($m^3\,mol^{-1}$)	$Y \times 10^{-12}$ (m^2)	V_a ($m^3\,mol^{-1}$)	R ($m^3\,mol^{-1}$)$\cdot$($m\,s^{-1}$)$^{1/3}$	S	R_A	Z ($kg\,m^{-2}\,s^{-1}$)
323.15 K										
Ethanol	23.237	60.294	3.787	15.073	11.940	20.395	614.596	2.647	1.000	808.966
Water	14.030	18.231	2.542	4.558	5.379	0.659	210.653	3.856	1.141	1523.686
Ethyl acetate	22.554	102.039	4.513	25.510	16.956	36.600	1029.293	2.566	1.142	886.004
298.15 K										
Ethanol	23.237	60.294	3.787	15.073	11.940	20.395	612.942	2.858	1.000	898.363
Water	14.030	18.231	2.542	4.558	5.379	0.659	206.689	3.743	1.160	1492.459
Ethyl acetate	22.554	102.039	4.513	25.510	16.956	36.600	1028.358	2.844	1.140	1017.570
288.15 K										
Ethanol	19.229	57.986	3.738	14.496	11.633	15.288	612.483	2.946	1.000	936.006
Water	13.777	18.029	2.533	4.507	5.339	1.506	204.853	3.666	1.169	1465.084
Ethyl acetate	17.919	97.189	4.441	24.297	16.414	25.297	1028.112	2.959	1.139	1072.939

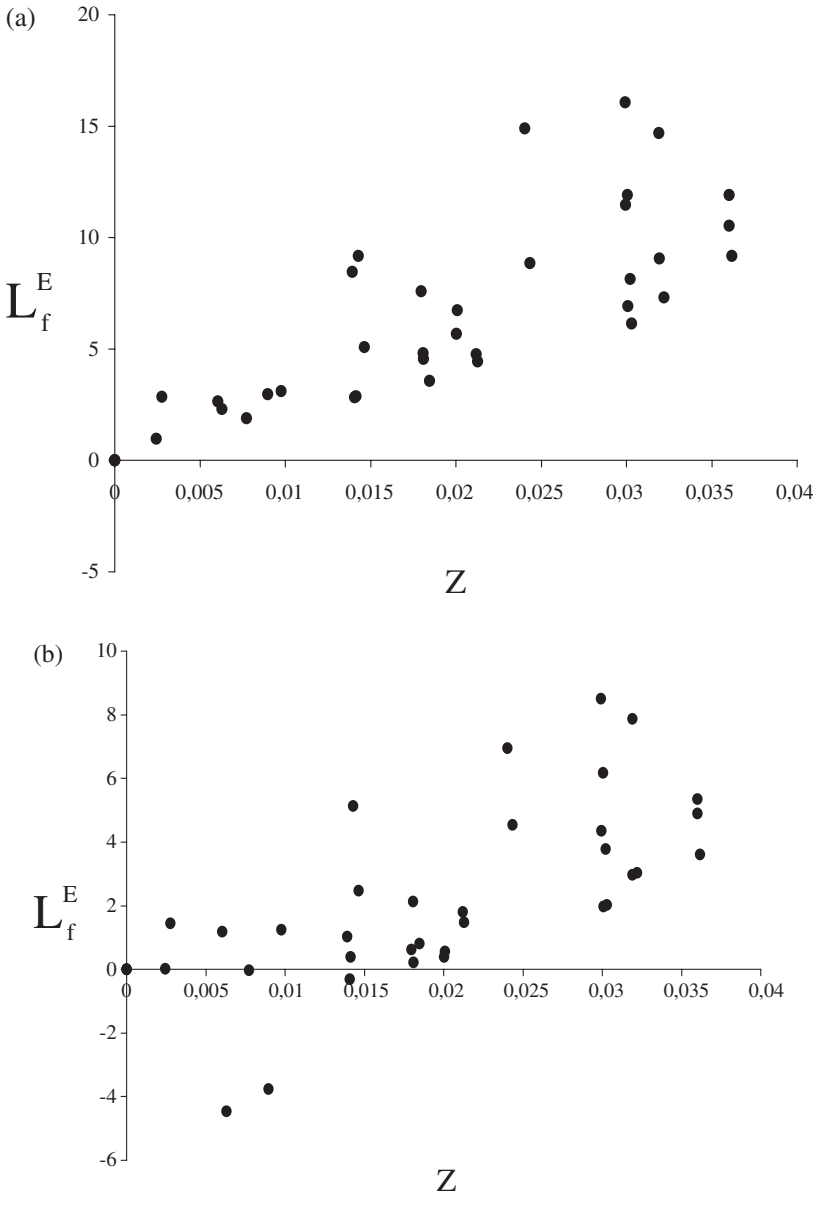

Figure 3. Curves of excess intermolecular free length for ethanol + water + ethyl acetate: (a) 323.15 K; (b) 298.15 K; (c) 288.15 K *vs.* z.

of water are displaced by increasing ethyl acetate in solution. An isoline of zero value exists where the compressibility of the three components are the same from the ethanol + water to the ethanol + ethyl acetate binary mixture. Only at a high concentration of ethanol, the negative values change their sign and the diagram shows positive values of hydration numbers. The negative hydration numbers reflect strong ternary interactions; this effect could be ascribed to the longer lifetimes of hydrogen bonds in equimolar ternary mixtures than in ethanol–ethanol or water–water environment.

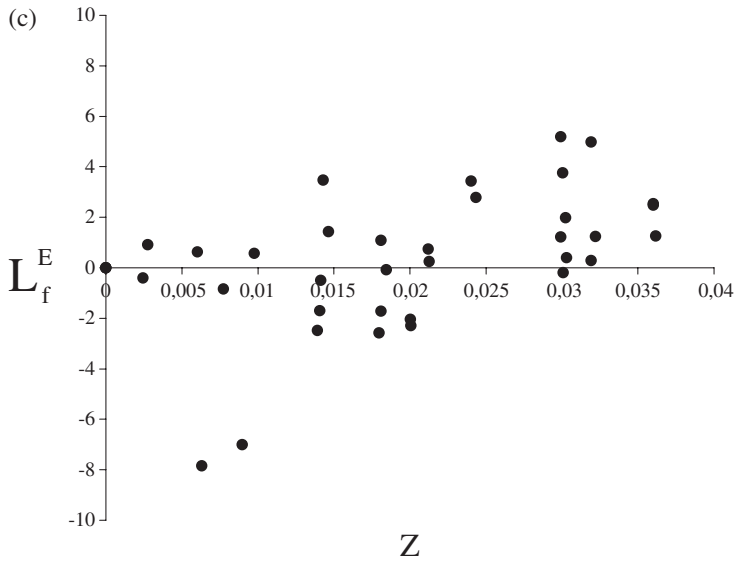

Figure 3. Continued.

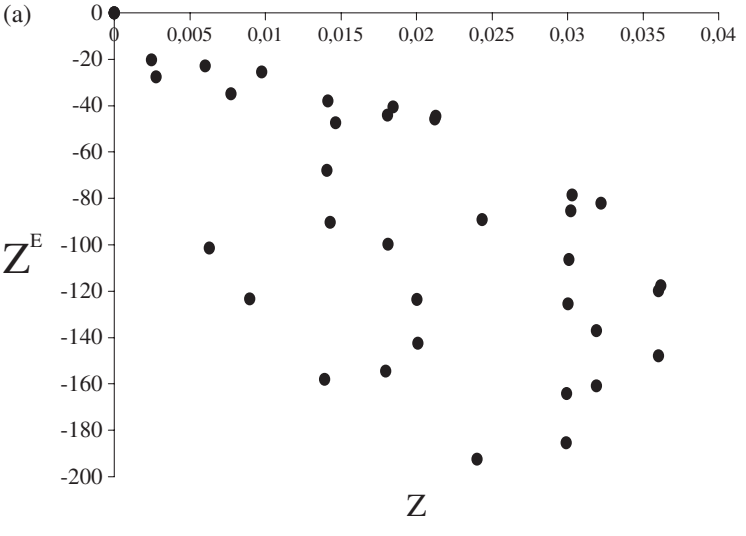

Figure 4. Curves of excess specific acoustic impedance for ethanol + water + ethyl acetate: (a) 323.15 K; (b) 298.15 K; (c) 288.15 K *vs.* z.

When the temperature is increased from 288.15 to 323.15 K, there is a corresponding rise in the ultrasonic velocity and then an increment in the entropy of the system, the strongest values being observed for the lowest temperatures.

3.3 *Estimation models*

Due to the strong dependence of design and optimization of chemical processes on computer calculations, the availability of accurate, simple and tested methods,

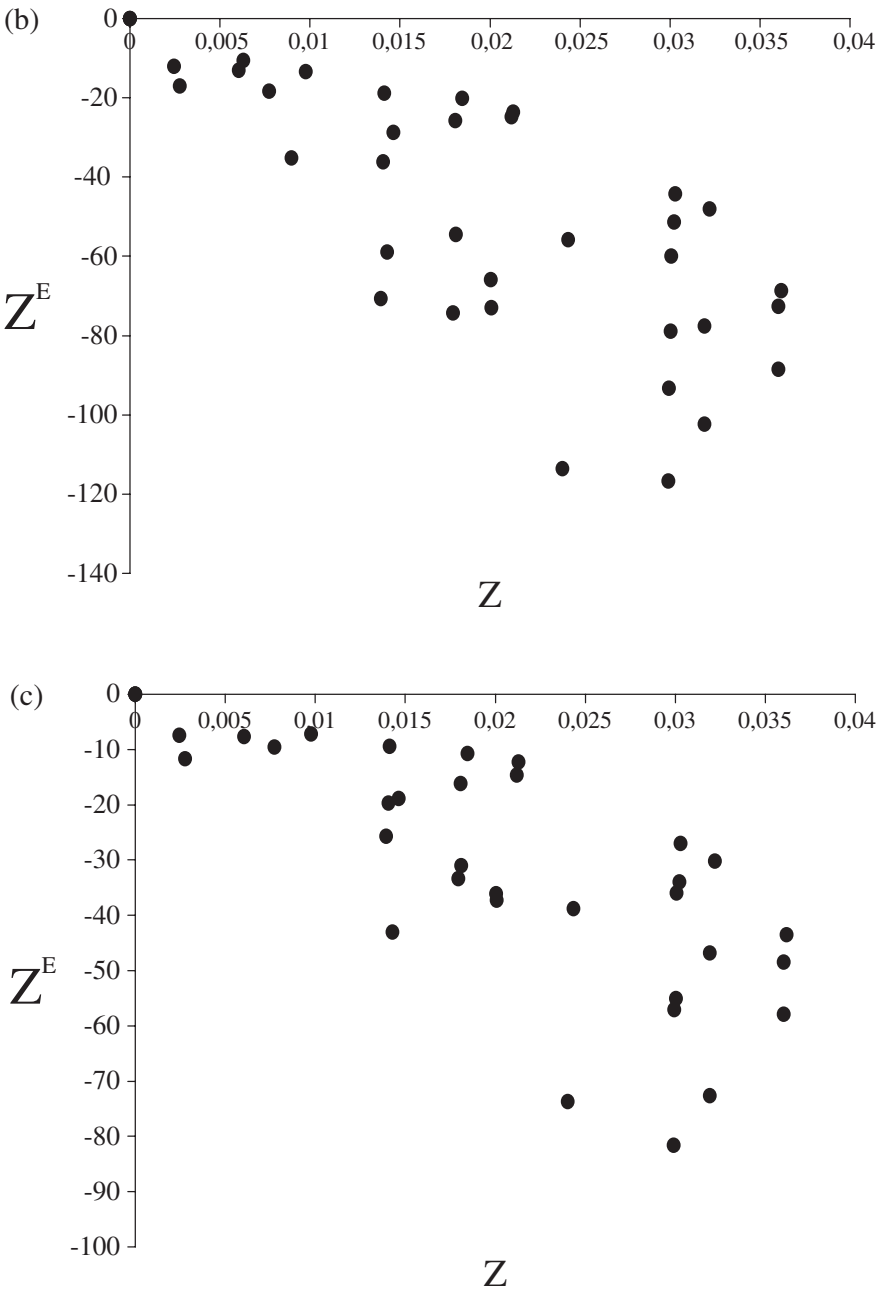

Figure 4. Continued.

as well as related parameters is of increasing relevance. The estimation of different thermodynamic properties of binary or multicomponent mixtures have been the subject of study of many researchers in recent years, applying different empirical or semiempirical models due to their interest in optimizing industrial equipment and understanding

the liquid mixture properties. Experimental data for the isentropic compressibility of the mixtures were compared with values determined by different mixing procedures. The models of Danusso and Nomoto (equations (19) and (20) [5,6]:

$$\kappa_S = \left(\frac{1}{M \cdot \rho}\right) \cdot \left(\sum_{i=1}^{N} \frac{n_i M_i}{\rho_i^2 u_i^2}\right) \tag{19}$$

$$\kappa_S = \left(\frac{1}{\rho}\right) \cdot \left(\frac{\sum_i^N n_i R_i}{\sum_i^N n_i u_i}\right)^{-6} \tag{20}$$

where $R = u^{1/3} \cdot \sum_i^N n_i V_i$, and Collision Factor Theory (CFT) [7,8] (equation (21)) and Free Length Theory (FLT) [9] (equation (22)) for the isentropic compressibilities were applied:

$$\kappa_S = \left(\frac{1}{\rho^3}\right) \cdot \left(\frac{M}{u_\infty \cdot \sum_i^N x_i S_s \cdot \sum_i^N x_i B_s}\right)^2 \tag{21}$$

$$\kappa_S = \left(\frac{L_f^2}{K^2}\right) \tag{22}$$

The Collision Factor Theory (CFT) is dependent on the collision factors among molecules as a function of temperature into the pure solvent or mixture. The pertinent relations in these calculations and its theoretical basis were described by the literature cited above. The collision factors (S) and the characteristic molecular volumes (B) of the pure solvents used in the CFT calculations were estimated by using the experimental ultrasonic velocities enclosed in this article, and the corresponding molar volumes [3]. These values could also be evaluated by means of the group contribution method proposed by Schaffs [16] when no experimental data are available.

The Free Length Theory estimates the isentropic compressibility of a mixture attending to the free displacement of molecules as a main function of temperature. In the last few years, different authors have compared the relative merits of the existing theories with the Free Length Theory (FLT), the FLT results in lower deviations of computed isentropic compressibilities from experimental values. The deviations of each procedure for the studied mixtures are gathered into table 5 by means of equation (5), and as expected, they increase as a consequence of rising temperatures. Considering the deviation of computed data, we arrive at the conclusion that the application of the Free Length Theory predicts experimental data extremely well

Table 5. Root mean square deviations for estimated isentropic compressibilities from experimental data for the ternary mixtures at range of 288.15–323.15 K.

Mixture	Danusso (equation (19))	Nomoto (equation (20))	CFT (equation (21))	FLT (equation (22))
Ethanol + water + ethyl acetate (323.15 K)	126.61	53.92	118.93	2.49
Ethanol + water + ethyl acetate (298.15 K)	92.71	53.35	56.06	1.58
Ethanol + water + ethyl acetate (288.15 K)	84.41	54.30	35.77	1.32

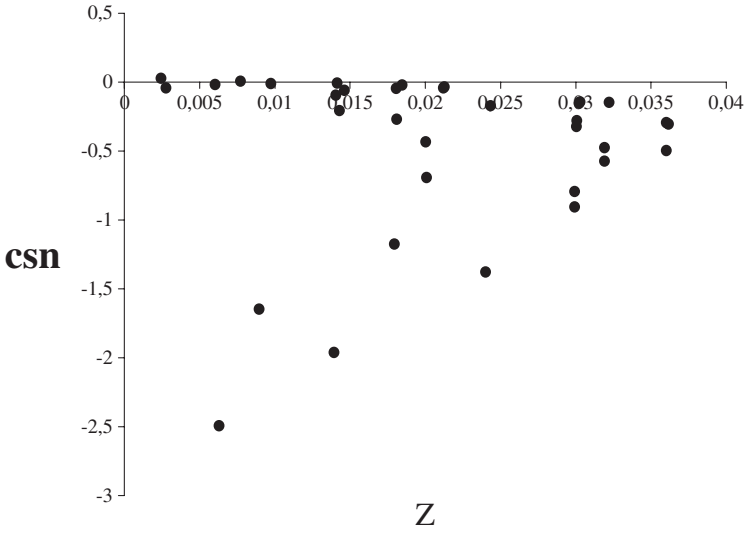

Figure 5. Compressibility hydration numbers for ethanol + water + ethyl acetate at 298.15 K.

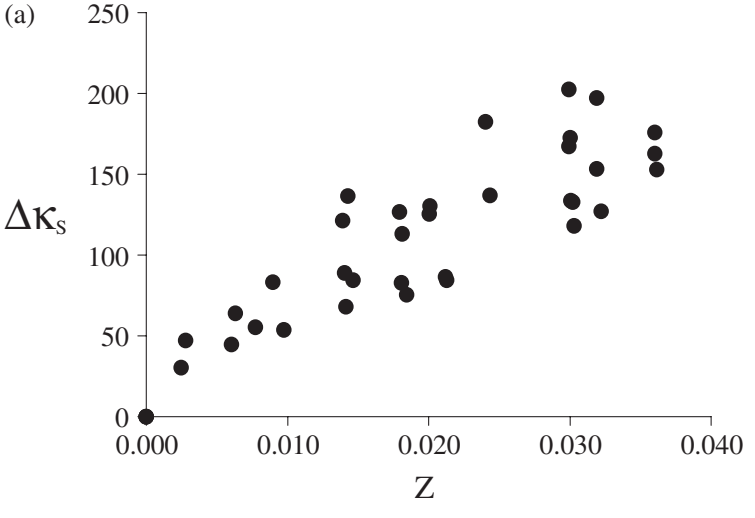

Figure 6. Curves of deviation from experimental data of the estimation by CFT for ethanol + water + ethyl acetate: (a) 323.15 K; (b) 298.15 K; (c) 288.15 K.

for all the studied mixtures, showing this procedure as an accuracy tool for isentropic compressibility data in these kind of systems (figures 5–7).

4. Results and conclusions

As it could be expected, attending to the molecular structure of solvents, three different trends of interaction could be observed: a hydrogen bond interaction dominates the ethanol + water mixture yielding to negative values of the derived property in the

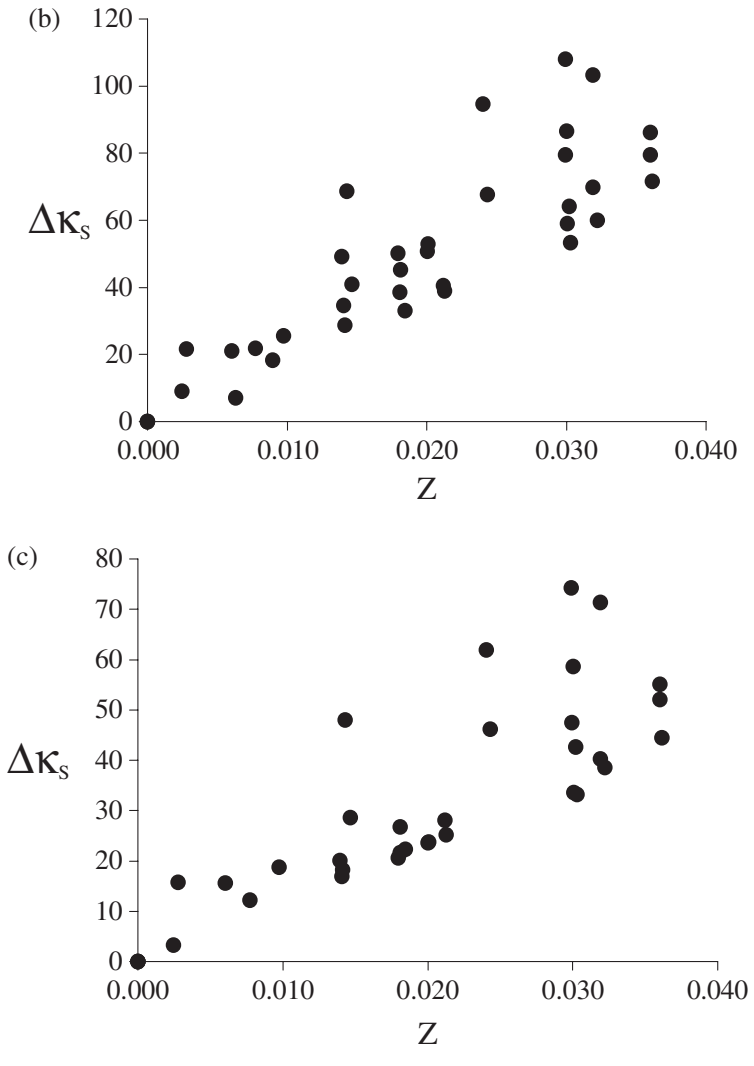

Figure 6. Continued.

corresponding pseudobinary mixture. Second, a phase splitting occurs in water + ethyl acetate mixtures when neither water nor ethyl acetate is the most abundant component. These facts are analyzed in recent experimental studies at different temperatures in ternary compositions [17]. And third, a strong contractive tendency for almost equimolar compositions occurs in the neighbourhood of the binodal curve (maxima of change of isentropic compressibility). The peculiar behaviour is conditioned mainly by the steric hindrance over the aliphatic end of the ester into the extremely ordered hydroxylic structure in such a way that diminution or increment of ester composition affects notably the contractive tendency and then the sign and magnitude of change of isentropic compressibility. In addition, as it occurs in volumetric properties of this

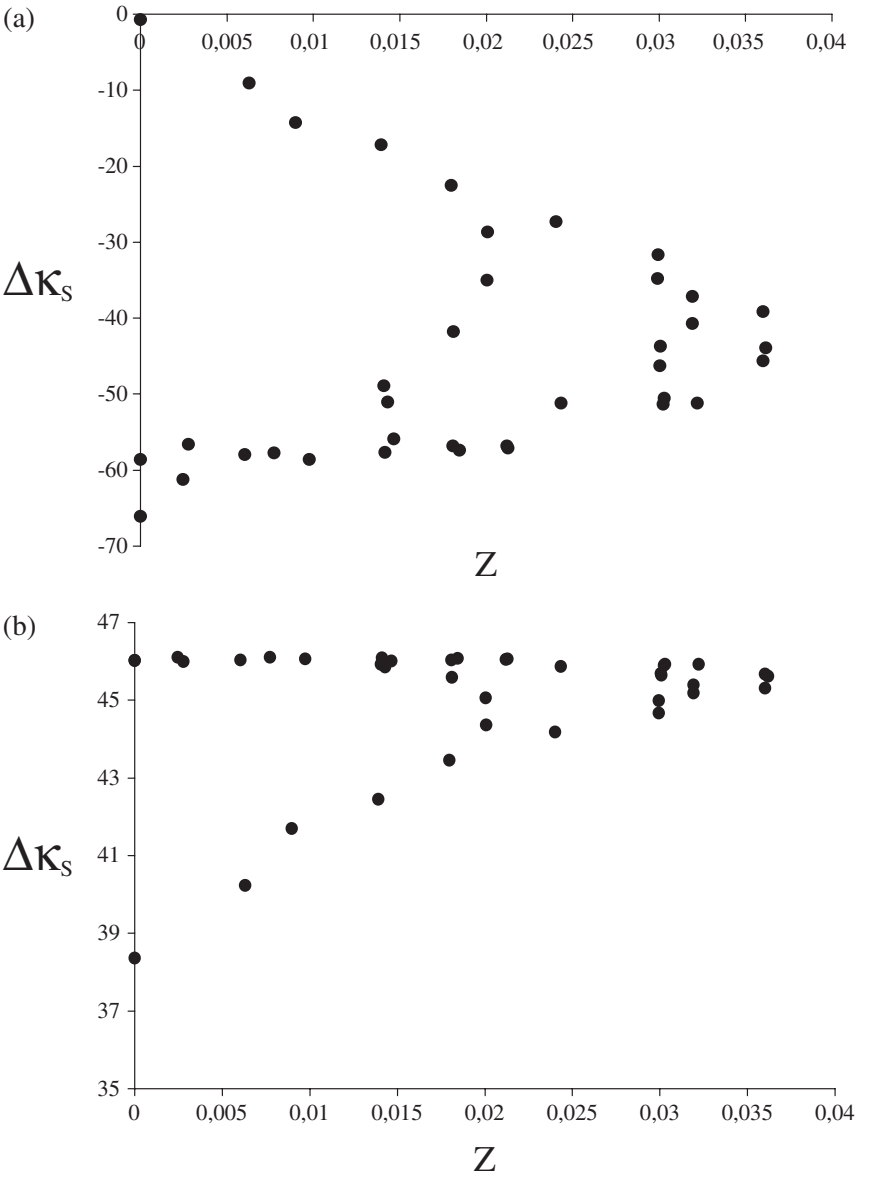

Figure 7. Curves of deviation from experimental data of the estimation by FLT for ethanol + water + ethyl acetate: (a) 323.15 K; (b) 298.15 K; (c) 288.15 K.

kind of mixtures [3], the most non-ideal trend is observed for the lowest temperatures showing positive derived magnitudes, so that the values of isentropic compressibilities are higher than ideal mixtures and then, a more rigid mixture. These results tally perfectly with previous studies [3,17], showing that ethanol is the key component for phase splitting (low values of ethanol produces liquid–liquid equilibria into the system) and ethyl acetate is the key component for the contractive character of the

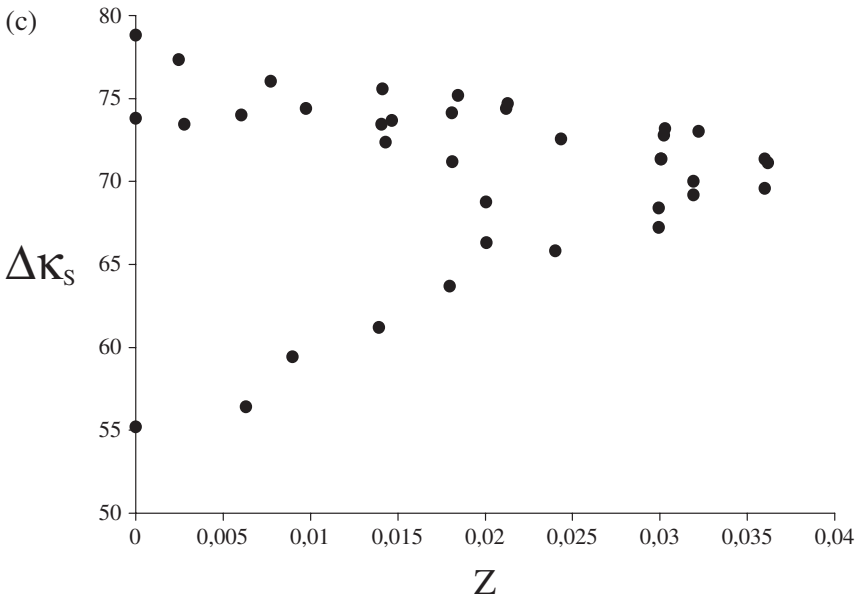

Figure 7. Continued.

mixture. Moreover, the high dilution or high concentration produces a diminution in the contractive trend. Temperature, in this case, deals towards diminution of negative values of change of isentropic compressibility, probably due to an increasing difficulty in the accomodation of the aliphatic end of the ester molecule. In the last few years, different studies have pointed out the special "iceberg structure" of hydroxyl short molecules, specially aqueous mixtures, and the intense modifications that this structure suffers as a function of composition modification. This special structure is specially sensitive to globular molecules with polar or slight polar groups (as ester group) and inert solvents, which are enclosed with difficulty. The aqueous dilution of ethyl ester shows an expansive trend, while phase splitting is not produced, due to the disruption of the polar interaction among water molecules by the inert diluent. This behaviour is extrapolated to near ternary compositions, such predominant interaction being attenuated by the composition increment of the third solvent (ethanol). The autoassociative behaviour of ethanol is the cause of contractive tendency with water (polar hydroxyl group) and slight polar-dispersive interaction molecule of ester. Water + ethyl acetate mixtures show a partial expansive trend because the polar difference is strong enough for phase splitting at the studied temperatures. Attending to this trend, it is not surprising to observe a symmetric attenuation towards diluted ternary compositions.

The mathematical structure of the equation (4) leads one to analyze the ternary contribution ΔQ_{ter} (simultaneous interactions among all compounds into mixture) in what is referred to as the shape and sign (figures 2(a), (b) and (c)). This contribution shows two important questions: firstly, the considerable contribution to the derived property by ternary molecular interactions, although it is a decreasing factor for higher temperatures; secondly, the approximately equimolecular maximum

in ternary contribution with only negative values for the highest studied temperature at rich *n*-hexane composition. Such a trend is normal due to the evolution of the physical property as a function of molar fraction. The partial rupture of alcohol + water close structure when the ester is introduced is reflected in the isentropic compressibility by a strong and continuous variation, from negative values, towards increasing values until it reaches a maximum. The solvation layer around the ethanol layer is dissolved faster as temperature rises, which may also be true for the whole set of ester functional family. A global weakening of intermolecular interactions is observed, which could be used to account for the isentropic compressibilities. Both facts help us understand the relative inaccuracy of the theoretical models in the estimation of these ternary values. Considering the complex interaction and the temperature dependence of phase splitting, this mixture was selected to test the ability of these models to predict multicomponent changes in isentropic compressibilities.

These models are, at least, of qualitative accuracy to predict ternary values of change of isentropic compressibility, showing the FLT to be lower deviation for the entire composition range. Deviations observed in the estimated ternary magnitude also show dependence on the temperature, and can be considered to be a satisfactory result for this model, supporting its validity as a predictive tool, having in mind the high non-ideality of the ternary mixture, where both associative and phase splitting phenomena occur.

Acknowledgements

Miguel Iglesias wishes to thank the Basque Country Government, Departamento de Educación, Universidades e Investigación, Dirección de Política Científica (Eusko Jaurlaritza, Hezkuntza, Unibertsitate eta Ikerketa Saila) for its support in his research.

References

[1] M. Gaiser, G.M. Bell, A.W. Lim, N.A. Roberts, D.B.F. Faraday, R.A. Schultz, R. Grob. *J. Food Eng.*, **51**, 27 (2002).
[2] J.M. Resa, C. Gonzalez, J.M. Goenaga, M. Iglesias. *J. Chem. Eng. Data*, **49**(4), 804 (2003).
[3] J.M. Resa, C. Gonzalez, J.M. Goenaga, and M. Iglesias, *J. Solution Chem.* (submitted for publication) (2004).
[4] I. Cibulka. *Coll. Czech. Chem. Comm.*, **55**(7), 1653 (1990).
[5] F. Danusso. *Atti Accad. Nazl. Lincei*, **10**, 235 (1951).
[6] O. Nomoto. *J. Phys. Soc. Japan*, **13**, 1528 (1968).
[7] R. Nutsch-kuhnkies. *Acustica*, **15**, 383 (1965).
[8] W. Schaffs. *Acustica*, **33**, 4, 272 (1975).
[9] B. Jacobson. *Acta Chemica Scandinavica*, **6**, 1485 (1952).
[10] *TRC Thermodynamic Tables* (Thermodynamic Research Center, Texas A&M University: College Station, TX) (1994).
[11] C. Gonzalez, M. Iglesias, J. Lanz, J.M. Resa. *Thermochimica Acta*, **328**, 277 (1999).
[12] O. Redlich, A.T. Kister. *Ind. Eng. Chem.*, **40**, 345 (1948).
[13] P. Bevington. *Data Reduction and Error Analysis for the Physical Sciences* (McGraw-Hill: New York) (1969).
[14] A. Gayol, M. Iglesias, C.G. Concha, J.M. Goenaga, C. Gonzalez, J.M. Resa. *Fluid Phase Eq.* (submitted for publication).
[15] J.M. Resa, C. Gonzalez, J.M. Goenaga, M. Iglesias. *J. Molecular Liq.* (submmitted for publication).

[16] D.W. Marquardt. *J. Soc. Indust. Appl. Math*, **2**, 431 (1963).
[17] W. Schaaffs. *Molekularakustic* (Springer Verlag: Bonn) (1963).
[18] J.M. Resa, C. Gonzalez, M. Iglesias, J.M. Goenaga, R.G. Concha. *J. Chem. Eng. Data* (submmitted for publication).